Atomic arrangement in the $c(2 \times 2)$ structure of Cl on Ag(100)

E. Zanazzi*† and F. Jona*
Department of Materials Science, State University of New York, Stony Brook, New York 11794

D. W. Jepsen and P. M. Marcus
IBM Research Center, P. O. Box 218, Yorktown Heights, New York 10598

(Received 10 March 1976)

A LEED (low-energy electron diffraction) structure analysis is described of the $c(2 \times 2)$ superstructure obtained by reacting a clean Ag(100) surface with Cl. Two of the structural models considered in the analysis produce encouraging agreement between theory and experiment for some LEED beams: the overlayer model with Cl adsorbed on the fourfold symmetrical hollows of the Ag(100) surface in the $c(2 \times 2)$ arrangement and the mixed-layer model with non-coplanar Ag and Cl atoms. The full analysis of 21 beams at three different angles of incidence and one azimuth, however, leads to rejection of the mixed-layer model and adoption of the simple overlayer model. Refinement of the structure with regard to several nonstructural parameters reveals an interference between the choice of the potential for the adsorbed Cl and the value of the distance d_z^S between overlayer and first substrate layer. For the proposed structure, $d_z^S = 1.72$ Å, corresponding to a hard-sphere Cl radius of 1.23 Å, but range of acceptable d_z^S values extends from 1.57 to 1.78 Å, depending on the Cl potential used in the intensity calculations.

I. INTRODUCTION

The purpose of the present work is the determination of the atomic arrangement in the $c(2\times2)$ structure formed by chemisorption of Cl on the (100) surface of Ag. Knowledge of such atomic arrangement may be helpful for an understanding of both the epitaxial relationships found in the growth of AgCl on Ag (Refs. 1, 2) and the mechanism by which Cl affects the oxidation of Ag,[3,4] a mechanism useful for the study of the catalytic properties of Ag.

Determination of the atomic arrangement in the $c(2\times2)$ surface layer has been done by the methods of LEED (low-energy electron diffraction) crystallography, i.e., by means of an analysis of the intensities of back-scattered low-energy electrons. Several structural models have been examined but only one has been found to produce satisfactory agreement with experiment. In this model, the Cl atoms are distributed on a simple overlayer and are located in the fourfold symmetrical hollows of the Ag (100) surface.

The structure analysis and its refinement generally require a study of the effects of nonstructural parameters upon the search for the "correct" structural model. In the present study, the choice of the potential turned out to be important for the precise determination of the distance between the overlayer and the first atomic layer of the Ag(100) substrate.

In Sec. II, we describe the pertinent experimental details. We present the results of the LEED structure analysis in Sec. III and discuss the effects of nonstructural parameters on the intensity calculations in Sec. IV. Then, in Sec. V, we draw the final conclusions applicable to the structure investigated.

II. EXPERIMENTAL

The Ag(100) $c(2\times2)$-Cl structure was prepared with the procedure developed and described by Rovida and Pratesi.[5,6] In particular, the substrate was a single crystal of Ag with purity 99.9999%, cut along the (100) plane with an accuracy better than 1°, and polished and etched in nitric acid prior to installation in the LEED chamber. The surface was cleaned *in situ* with argon-ion bombardments followed by annealing treatments in vacuo. It was then exposed for a few minutes (1–5 min) to pressures of the order of 100 mTorr of dichloroethane ($C_2H_4Cl_2$, ethylidene chloride) at about 150 °C. The exposure took place in a movable isolation chamber as described elsewhere.[5] The dichloroethane gas decomposes on the hot substrate surface and leaves thereon only Cl, as confirmed by Auger electron spectroscopy (AES).

The following experimental observations are likely to be of interest. The Ag (100) surface appeared very well crystallized, prior to exposure to dichloroethane, as indicated by small and sharp diffraction spots and a highly contrasted LEED pattern. The absorbed Cl layer appeared to be unstable under the action of the electron beam from the AES gun: Only with primary energies lower than about 1300 eV, for currents of the order of 100 μA, was it possible to slow down the electron desorption of Cl sufficiently for meaningful AES

observations. However, no effect on the Cl adlayer was observed by the LEED-gun electrons over periods of several hours. Finally, observation of the $c(2\times2)$ structure was always accompanied by the observation of weak "maverick" beams caused by faceting. These beams disappeared with the $c(2\times2)$ structure every time the substrate surface was cleaned. The obvious concern about the possible effects of the faceting beams upon the LEED intensity data needed for structure analysis of the $c(2\times2)$ structure was relieved by the following observations: (i) The intensities of the faceting beams were so low that, while they could be detected by the naked eye, they could not be seen through the optics of the spot photometer used for collection of LEED spectra intensities. (ii) No changes (shoulders, bumps) were observed in the measured LEED intensity curves whenever one or more faceting beams were known to enter or leave the field of view interrogated with the spot photometer.

The intensity spectra were recorded, as implied above, by measuring with a spot photometer the brightnesses of the corresponding LEED spots on the fluorescent screen of a display-type LEED equipment. Each recorded spectrum was then (a) corrected for the background by subtracting a uniform background-intensity curve obtained by interpolation of data points measured on the fluorescent screen in the immediate vicinity of the corresponding diffraction spot at the minima of the latter; (b) corrected for the appropriate contact-potential difference; (c) normalized to constant incident electron current; and (d) converted to units of electron current by suitable calibration of the response of the fluorescent screen and spot-photometer combination.

Conditions for normal incidence and minimization of the residual magnetic field were established and tested by comparing the intensity spectra of degenerate beams. A total of 21 LEED spectra were recorded up to about 150 eV of incident electron energy for three values of the angle of incidence θ and one value of the azimuth angle ϕ. As customary, θ is defined as the angle between the incident beam $\vec{k}$ and the normal to the substrate surface, and is always positive. The definition of the azimuthal angle ϕ requires unique identification of the reciprocal lattice axes $\vec{k}_x, \vec{k}_y, \vec{k}_z$ and is, therefore, tied to the indices assigned to the LEED beams. In order to make identification and assignment unambiguous, more precise instructions are necessary than have been provided in the literature so far. The steps are as follows: (1) Choose the unit mesh on the surface net; (2) Choose the z axis as directed from the surface *into* the crystal; (3) Choose x and y axes in the surface plane in such a way as to form a right-handed system; (4) Find the directions and signs of the reciprocal-lattice axes $\vec{k}_x$, $\vec{k}_y$, and $\vec{k}_z$; (5) Draw the vector $\vec{k}_{\parallel}$ that represents the projection on the surface of the incident wave vector $\vec{k}$; (6) Define the azimuthal angle ϕ, when looking in the direction of positive z, as the angle going from $\vec{k}_{\parallel}$ to $\vec{k}_x$, or when looking in the direction of negative z, as the angle going from $\vec{k}_x$ to $\vec{k}_{\parallel}$—in either case the positive direction is defined as counterclockwise; and (7) In the most common display-type LEED equipment (involving sample location between fluorescent screen and observer) the LEED pattern observed will be the reciprocal net obtained above but viewed from the tip of the $\vec{k}_z$ axis, i.e., looking in the direction of negative z. In the present work, the unit mesh chosen was the primitive square mesh of the Ag (100) surface. The following spectra were recorded and used in the analysis discussed in Sec. III; (a) at $\theta=0°$; $\bar{1}0, \bar{1}\bar{1}, \frac{1}{2}\frac{1}{2}, \frac{1}{2}\frac{3}{2}$; (b) at $\theta=10°$ and $\phi=29.5°$: $00, \bar{1}0, 0\bar{1}, \bar{1}\bar{1}, \frac{1}{2}\frac{1}{2}, \frac{1}{2}\frac{\bar{1}}{2}, \frac{\bar{1}}{2}\frac{1}{2}, \frac{\bar{3}}{2}\frac{1}{2}, \frac{1}{2}\frac{\bar{3}}{2}, \frac{\bar{3}}{2}\frac{\bar{3}}{2}$; (c) at $\theta=20°$ and $\phi=29.5°$: $00, \bar{1}0, 0\bar{1}, \bar{1}\bar{1}, \bar{2}0, \frac{\bar{1}}{2}\frac{1}{2}, \frac{\bar{1}}{2}\frac{\bar{1}}{2}, \frac{\bar{3}}{2}\frac{\bar{1}}{2}$. The unusual value of the azimuth ϕ is due to the fact that the sample holder used in this study did not allow variations of ϕ *in situ*. The pertinent ϕ value was measured on a photograph of the LEED pattern.

III. STRUCTURE ANALYSIS AND RESULTS

The calculations of LEED intensities for the chosen structural models were done with the layer-KKR (Korringa-Kohn-Rostoker) method.[7] A total of 58 (29 integral-order and 29 fractional-order) beams and 8 phase shifts were used for the description of the electron wave function. The following structural models were investigated:

(a) Simple overlayer (i.e., adsorbed atoms *above* the substrate atoms) with Cl atoms on the fourfold symmetrical hollows of the Ag (100) surface in the $c(2\times2)$ arrangement [Fig. 1(a)].

(b) Mixed Cl-Ag layer, with each of the Cl and Ag atoms on fourfold symmetrical sites of the underlying (100) plane of Ag atoms [Fig. 1(b)]. The distance between the plane through the centers of the Cl atoms and the plane through the centers of the surface-layer Ag atoms (referred to below as the Cl-Ag intralayer distance) was varied from −0.16 Å (Cl farther from the substrate) to 0 Å (coplanar Cl-Ag mixed layer) and, in succession, +0.08, 0.16, 0.24, 0.32, and 0.48 Å (Cl atoms closer to the substrate).

(c) Simple overlayer with the Cl atoms on the bridge sites in the $c(2\times2)$ arrangement [Fig. 1(c)]. This model allows two domains, rotated 90° from one another, which were assumed to be equally

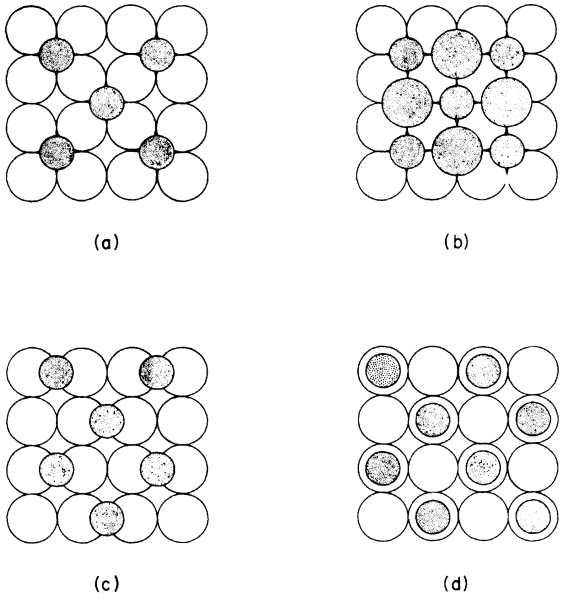

FIG. 1. Schematic models of the $c(2\times2)$ structures assumed for the calculations. (a) Overlayer with Cl in fourfold symmetrical sites; (b) Ag-Cl mixed layer; (c) Overlayer with Cl in bridge sites (one of two domains); (d) Overlayer with Cl in top sites. Shaded circles: overlayer or mixed-layer atoms. Open circles: Substrate Ag atoms.

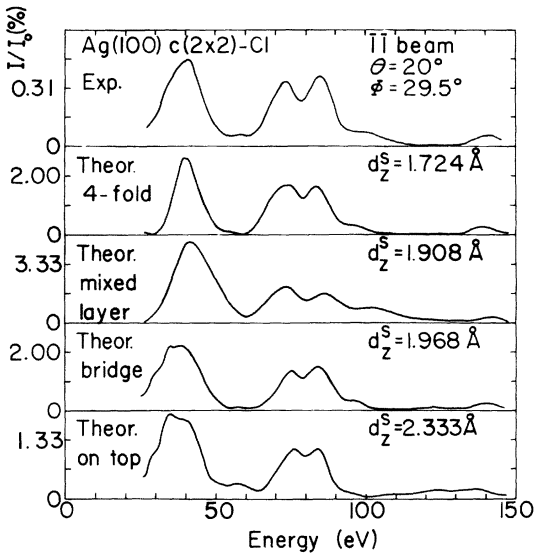

FIG. 2. Comparison between experimental spectrum (top curve) and the most appropriate theoretical spectrum for each of the structural models depicted in Fig. 1, for the $\bar{1}\bar{1}$ beam at $\theta = 20°$, $\phi = 29.5°$. The parameter d_z^S denotes the distance between the plane through the centers of the Cl atoms and the plane through the centers of the Ag atoms in the first substrate layer. In the mixed-layer model, the Cl plane is lower (closer to the substrate) than the Ag plane by 0.24 Å, while d_z^S denotes the distance of the Ag plane from the first substrate layer.

represented on the surface. Accordingly, the intensity calculations were carried out separately for each domain type and then averaged with equal weight.

(d) Simple overlayer with the Cl atoms directly on top of underlying Ag atoms in the $c(2\times2)$ arrangement [Fig. 1(d)].

For all models investigated the interplanar distance d_z^S between the top atomic layer (or double layer in the case of the mixed-layer model) and the first substrate layer was varied over a reasonably wide range. This variation had marked effects on some spectra, hardly any on others.

Some of the calculated spectra were found to be in reasonable agreement with experiment for any and all structural models. An example of this fact is the $\bar{1}\bar{1}$ spectrum at $\theta = 20°$, $\phi = 29.5°$ depicted in Fig. 2. This spectrum is also notably sensitive to the d_z^S distance between superstructure and substrate, as can be seen in Fig. 3. This sensitivity allows us to choose, for each model, the d_z^S value that yields the best correspondence with experiment. For the mixed-layer model, we show in Fig. 2 and all following figures only the spectra calculated for an intralayer distance of 0.24 Å, which provided the best agreement with experiment, although variations of up to ±30% around this value caused only minor changes in the intensity curves.

Many of the calculated spectra, on the other hand, require the elimination of the bridge and top-site models [(c) and (d) above], and restrict the choice to the simple overlayer with Cl in the fourfold sites and to the mixed-layer model. Examples of these facts are the $\bar{2}0$ and the $\frac{3}{2}\frac{1}{2}$ beams at $\theta = 20°$, $\phi = 29.5°$, depicted in Figs. 4(top) and 4(bottom), respectively.

In order to make a meaningful choice between overlayer and mixed-layer models, it is necessary to examine all other spectra that have been measured experimentally (Figs. 5 and 6). For many beams, in fact, the agreement between observed and calculated spectra is roughly of the same quality, although the overlayer model is always at least slightly favored. For some beams, the mixed-layer model is definitely in disagreement with experiment and must, therefore, be discarded; see, e.g., the $\frac{1}{2}\frac{3}{2}$ spectrum at $\theta = 0°$, the $\frac{1}{2}\frac{1}{2}$ at $\theta = 20°$, $\phi = 29.5°$, and for several non-negligible details the 00 and the $\frac{1}{2}\frac{1}{2}$ beams at $\theta = 20°$, $\phi = 29.5°$.

For some spectra the correspondence between observations and calculations is not excellent even for the fourfold overlayer model, especially for some details. It should be noted, however, that

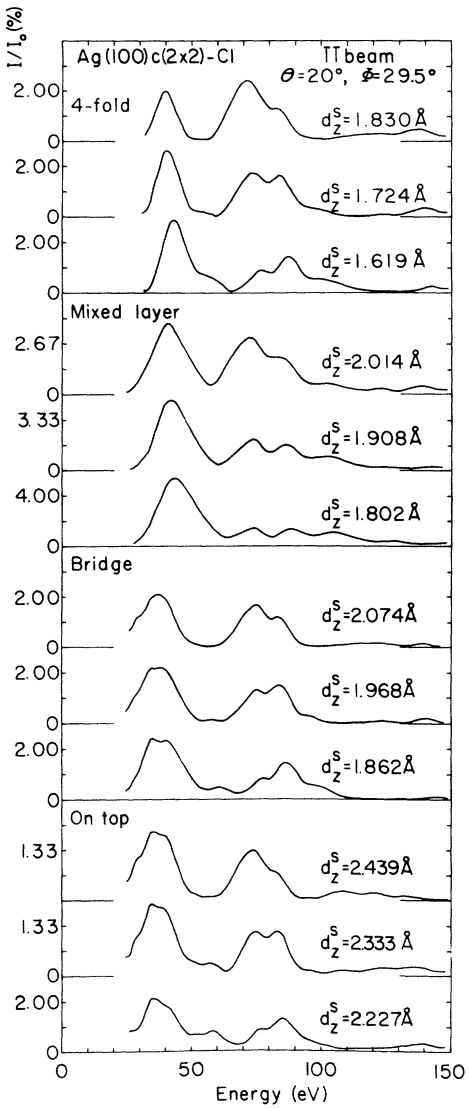

FIG. 3. Dependence upon d_z^S of the $\bar{1}\bar{1}$ spectra at $\theta=20°$, $\phi=29.5°$ calculated for each of the structural models depicted in Fig. 1.

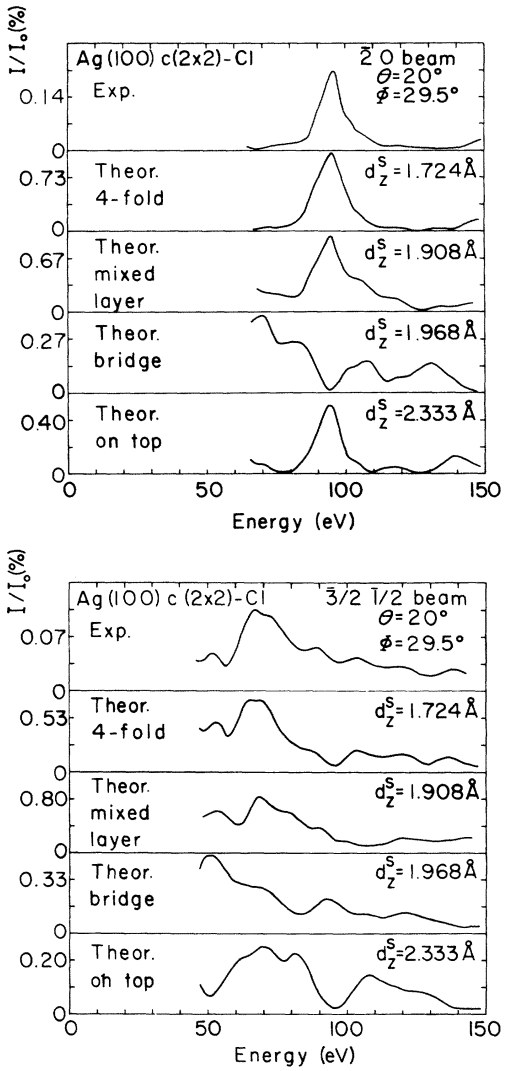

FIG. 4. $\bar{2}0$ (upper box) and $\bar{\frac{3}{2}}\bar{\frac{1}{2}}$ (lower box) spectra at $\theta=20°$, $\phi=29.5°$ as observed (top curves) and calculated for each of the structural models depicted in Fig. 1.

the corresponding beams have in general very low intensities—about 10–20 times lower than those of the most intense beams. For such weak beams experimental and calculational inaccuracies become very important. In general, the ratio between calculated and observed intensities fluctuates between 10 and 20, in line with the present trend in LEED crystallography.

No marked improvements in the overall agreement between theory and experiment can be obtained even by varying the interplanar distance between first and second *substrate* layers by as much as ±10%. Neither does the variation of this structural parameter affect the choice of the model that provides the best overall agreement with experiment.

We conclude, therefore, that the correct model for the Ag(100) $c(2\times 2)$ – Cl structure investigated here is the overlayer of Cl atoms in the fourfold symmetrical sites, with interplanar distance between Cl and first Ag layers of $d_z^S=1.72$ Å.

IV. EFFECTS OF THE NONSTRUCTURAL PARAMETERS

The results presented above have been obtained with the following values of the nonstructural parameters: inner potential $V_0=8$ eV, for both the surface layer and the bulk ($V_0=10$ eV for the mixed layer); imaginary part of the potential $\beta_B=4$ eV

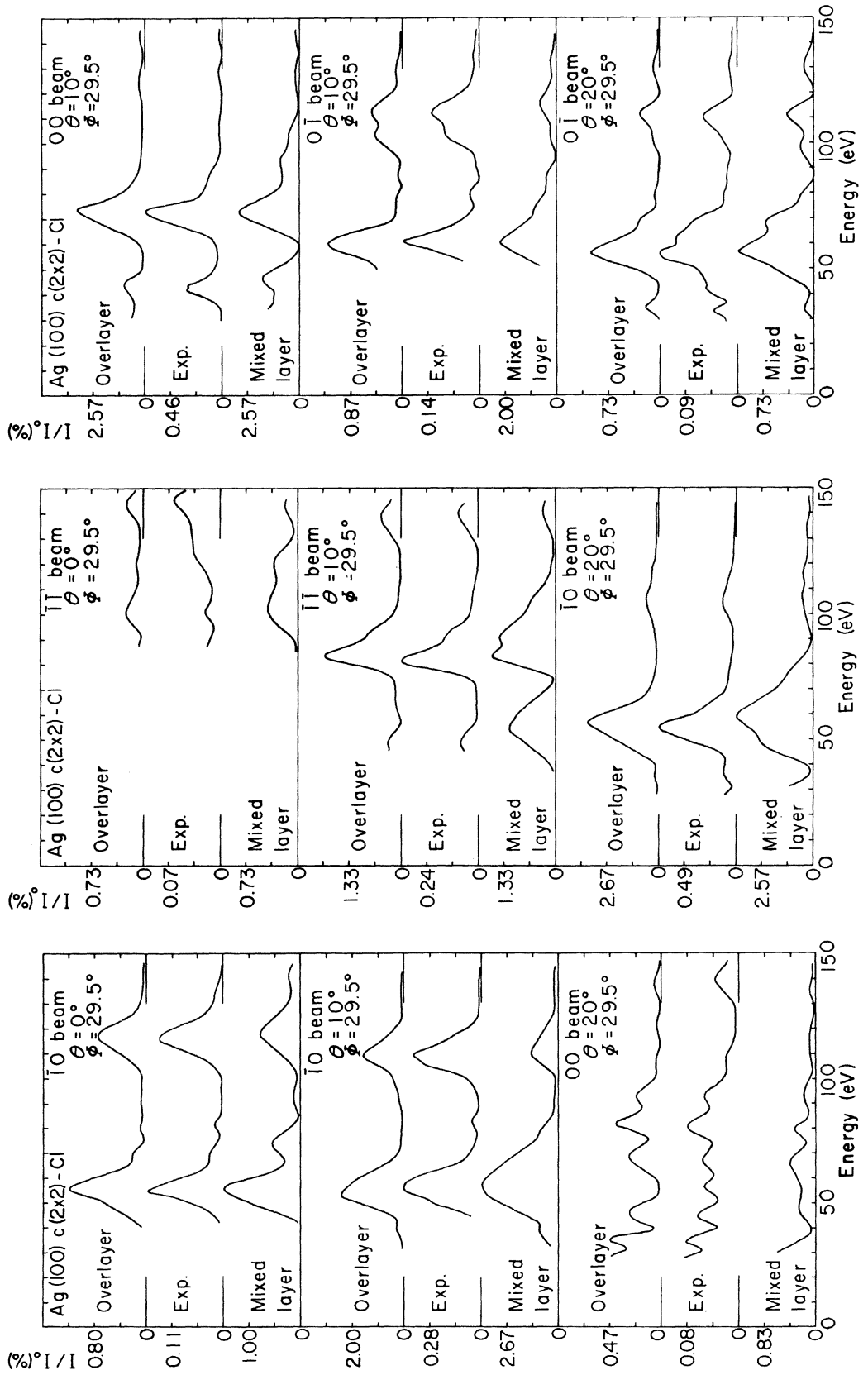

FIG. 5. Comparison between experiment (middle curve in each panel) and theories for the fourfold overlayer model (upper curve in each panel) and for the mixed-layer model (lower curve in each panel): integral-order beams for $\theta = 0°$, $\theta = 10°$, $\theta = 20°$, $\phi = 29.5°$.

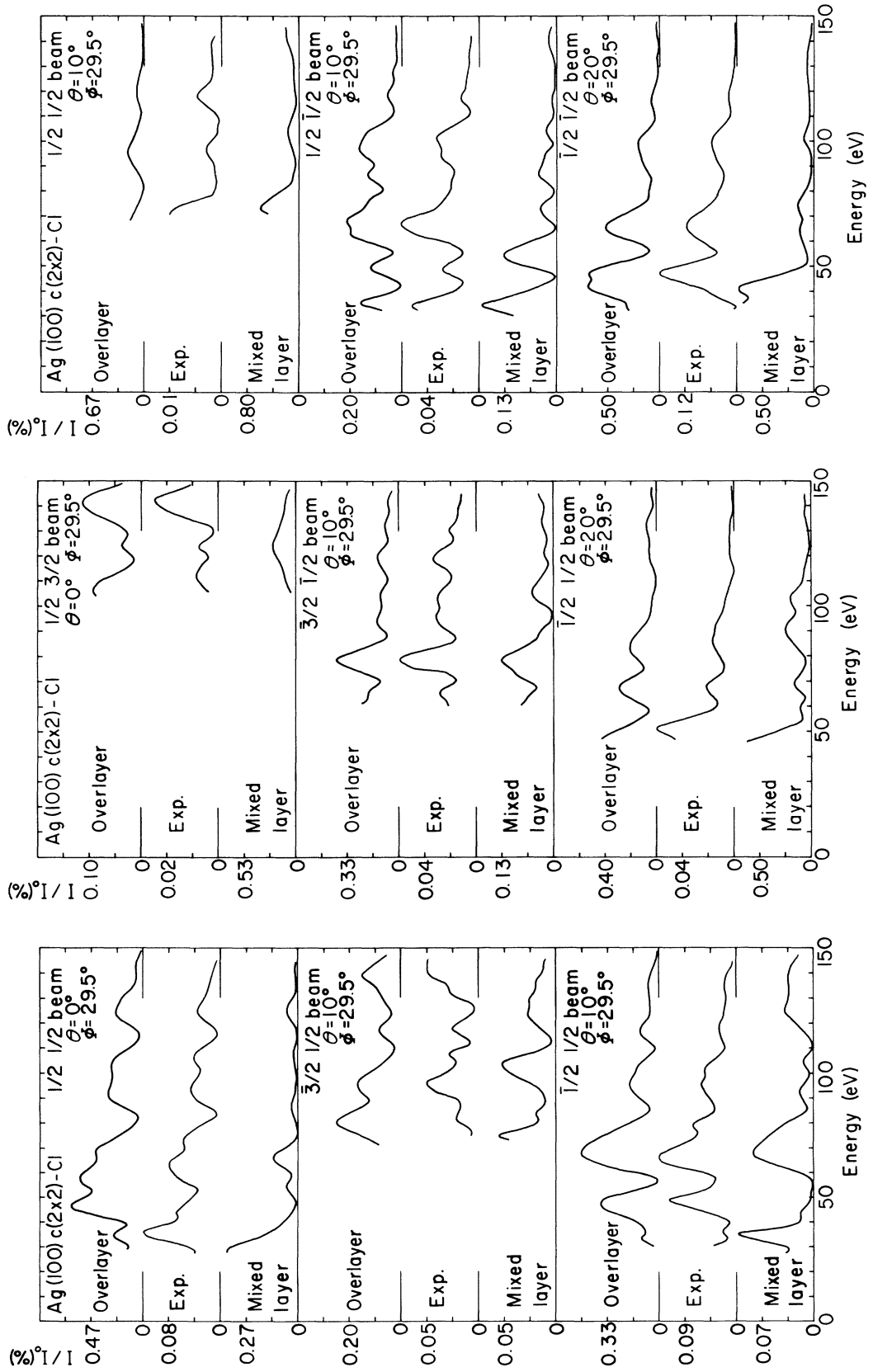

FIG. 6. Comparison between experiment (middle curve in each panel) and theories for the fourfold overlayer model (upper curve in each panel) and for the mixed-layer model (lower curve in each panel): fractional-order beams for $\theta = 0°$, $\theta = 10°$, $\theta = 20°$, $\phi = 29.5°$.

for the bulk and $\beta_S = 2.5$ eV for the surface layer; root-mean-square amplitude of atomic vibrations $(\langle u^2 \rangle)^{1/2} = 0.155$ Å, for both the surface layer and the bulk.

However, in the course of the analysis we have investigated the effects of changes in the nonstructural parameters. We give in the following the results of such investigations.

The root-mean-square amplitude $(\langle u_S^2 \rangle)^{1/2}$ of the surface atoms was varied from 0.110 to 0.220 Å (corresponding to $\langle u_S^2 \rangle$ varying between $0.5\langle u_B^2 \rangle$ and $2\langle u_B^2 \rangle$, with $\langle u_B^2 \rangle = 0.024$ Å^2 as the mean square amplitude of the bulk atoms). This variation resulted primarily in changes of the absolute intensities without marked changes in shapes or relative intensities within each spectrum.

Variation of the β_S and β_B values affects also the absolute intensities but may separate and resolve some adjacent peaks as well. We have also tried energy-dependent values of both β_S and β_B similar to those used in the analysis of the structure of the clean Ag (100) surface.[8] There is no doubt that a systematic search in this direction, combined with an energy-dependent inner potential, would bring about a general improvement of the correspondence between calculations and observations. However, such parameter variations appear to be rather artificial and whatever attempts we have made convinced us that this approach is not likely to lead us to a different choice of structural parameters, i.e., to a different structure.

Much more important for the precise determination of the surface structure is a variation of the potential of the adsorbed atoms. Such a potential was constructed, as customary, from the atomic charge densities of Cl with the atoms arranged in a fictitious bcc lattice. While in general this procedure produced satisfactory and unambiguous results, and the value of the lattice parameter of the fictitious bcc lattice was found to be rather inconsequential,[9-11] in the present case the limits of arbitrariness in the choice of the latter value produced a notable uncertainty in the structural parameters. The lower limit was chosen as the case in which the nearest interatomic distance in the fictitious bcc structure is equal to a mean value of the Cl-Ag distances found in a number of known compounds: This choice led to the value 0.93 Å for the muffin-tin radius of Cl. The upper limit involved a nearest interatomic distance in the fictitious bcc lattice somewhat larger than the Cl-Ag distance found in the structure reported above: This choice led to the value 1.325 Å for the muffin-tin radius of Cl. The effect of using Cl potentials calculated with the lower and the upper limits of the muffin-tin radius is shown in Fig. 7 for the $\overline{11}$ beam at $\theta = 20°$, $\phi = 20.5°$. As we mentioned above, this beam allows an unequivocal choice of the interplanar distance d_z^S between overlayer and first substrate layer for a given choice of the potential. We see in Fig. 7 that equally good agreement between theory and experiment is obtained with the two different potentials for two different values of d_z^S; i.e., $d_z^S = 1.57$ and 1.78 Å, respectively. With intermediate values of the Cl muffin-tin radius we obtained satisfactory agreement with experiment for correspondingly intermediate values of d_z^S. In particular, the results reported above (Figs. 2–6) were obtained with a potential calculated for a Cl muffin-tin radius of 1.23 Å. The reasons for this choice will be explained below.

It should be noted that qualitatively similar effects of the choice of Cl potentials were found in the mixed-layer model as well. In no case, however, was the mixed-layer model ever favored with respect to the fourfold overlayer model.

V. CONCLUSIONS

The solution of the present structure analysis as a simple fourfold site overlayer may not be surprising with respect to the other two simple overlayer models considered (bridge and top sites) but is somewhat puzzling vis-à-vis the mixed-layer model. In fact, the conditions under which the $c(2\times 2)$ structure was attained, in particular, the relatively high dichloroethane pressure and the high substrate temperature during chemisorption with the ensuing high mobility of Ag, would have led one to expect the formation of a mixed layer more probably than that of an adsorbed overlayer. Among other things, the mixed layer could have represented a slightly distorted plane of AgCl

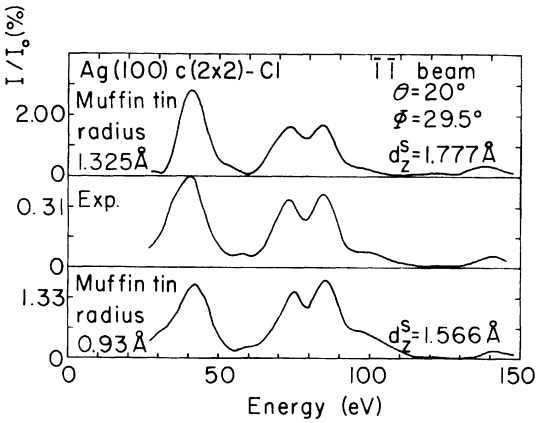

FIG. 7. Comparison between experiment (middle curve) and spectra calculated for the fourfold overlayer model with different Cl potentials: $\overline{11}$ beam at $\theta = 20°$, $\phi = 29.5°$. d_z^S is the distance between overlayer plane and first substrate layer.

(Ref. 5) and, as such, the first layer of epitaxial growth of AgCl over Ag. In the light of the results reported herewith, such a growth must rather be thought of as starting from small nuclei or islands which, however, must have had very small dimensions indeed if they were present at all on our surface during our observations.

The comparison between calculated and observed spectra, carried out for a large number of beams, reveals an agreement that is for some beams excellent, according to the standards presently prevailing in LEED crystallography, and for other beams only satisfactory. The observed discrepancies may be attributed to less than optimum values of nonstructural parameters. The intensities, on the other hand, are only in agreement in a relative, not absolute, sense. In general, as we mentioned above, the experimental intensities are smaller than the calculated ones by a factor fluctuating between 10 and 20. Such discrepancies are commonly observed in LEED crystallography and are rather vaguely attributed to irregularities of the substrate surface. In the present case, however, the high quality of the LEED pattern observed speaks rather against surface roughness and more in favor of either experimental errors in the normalization process or/and calculational inaccuracies with respect to nonstructural parameters such as the mean square amplitude of surface vibrations and the imaginary part of the potential.

It is worth noting that a convincing choice between overlayer and mixed-layer models could only be done on the basis of a large number of data. This fact on the one hand emphasizes once more the need for large data bases (i.e., as large as possible a number of beams) in order to carry out reliable surface structure analyses, and on the other reaffirms the relatively low sensitivity of low-energy electrons to the details and the population of superstructures.

An important, although unwelcome, result of the present study is the role played by the adsorbate potential in establishing the values of structural parameters. As far as we know, this is the first time that such a pronounced sensitivity as described above is observed in LEED crystallography.[10,12,13] It should also be noted that the absolute values of scattered intensities are affected by the choice of the potential, which, therefore, joins the other possible causes mentioned above of quantitative discrepancies between theory and experiment.

As it is sometimes instructive, in the study of surface structures, to think in terms of hard-sphere models, it is important to realize that the different structural parameters suggested by different Cl potentials imply different radii of chemisorbed Cl—if the atomic radius of Ag is maintained fixed at 1.44 Å, i.e., equal to one half of the nearest interatomic distance in bulk Ag. Figure 8 depicts the hard-sphere models for the two structures that were found using the Cl potentials calculated with the extreme values of the muffin-tin radius as defined above; and for the structure that was found on the basis of the results depicted in Figs. 2–6, the Cl muffin-tin radii (MTR) in the three cases being, respectively, 0.93, 1.325, and 1.23 Å. We see from Fig. 8, as well as from Table I, that by using a MTR of 0.93 Å we obtain a hard-sphere radius (HSR) of 1.13 Å which is obviously larger than the MTR. Hence, in this case the regions of space in which the potentials of Cl and Ag have spherical symmetry are *not* in contact with one another. In the other extreme case, on the other hand (MTR, 1.325 Å; HSR, 1.26 Å),

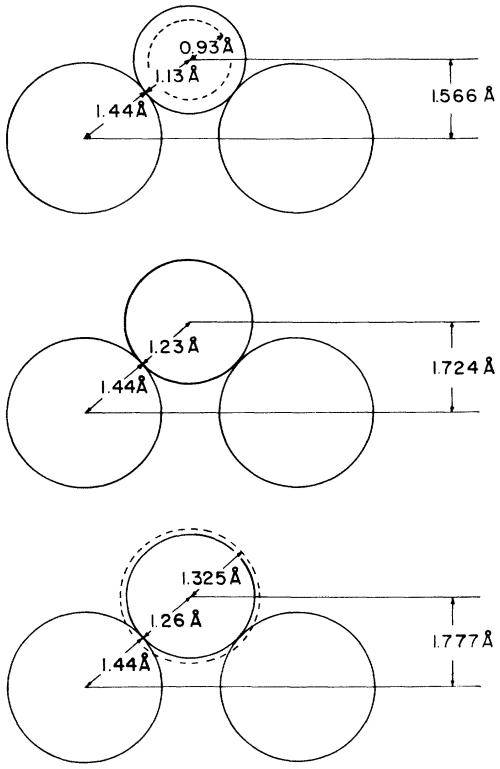

FIG. 8. Hard-sphere model of the Ag(100) $c(2 \times 2)$-Cl structure: cross section with a plane perpendicular to the surface passing through a Cl atom (small circles) and its two nearest-neighbors Ag atoms (large circles). Solid circles represent hard-spheres, dashed circles represent muffin-tin spheres for the atoms indicated. Top and bottom figures refer to the extreme values of muffin-tin radius chosen as described in the text. The middle figure corresponds to the case in which the muffin-tin radius equals the hard-sphere radius.

those same regions of space overlap one another. Keeping in mind the procedure usually followed for the calculation of self-consistent potentials in bulk elemental crystalline solids, in which the MTR is put equal to the HSR, we thought it may be reasonable to choose the MTR of Cl in such a way that in the hard-sphere model of the $c(2\times 2)$ structure the Cl and Ag atoms are just in contact with one another, i.e., to choose the MTR equal to the HSR. This is indeed the case for the Cl potential that we have used to calculate the spectra depicted in Figs. 2–6; i.e., both the MTR and the HSR are equal to 1.23 Å. It is worth noting that this value of the MTR can be found by linear interpolation from the two extreme values defined above and listed in Table I. This choice of the MTR also appears to be reasonable on qualitative physical grounds. In fact, it is somewhat smaller than half the actual distance between Cl and Ag in our overlayer structure, thus on the one hand taking into account the fact that the nearest neighbors of Cl are Ag atoms (hence the electron density around each Cl in the overlayer is larger than if it were surrounded by Cl atoms only), but on the other hand not too much smaller than that value (thus taking into account the fact that the electron density around a Cl atom in the overlayer is smaller than it would be if this atom were in the bulk rather than on the surface). Finally, we note that the HSR radius 1.23 Å of Cl found in our structure is somewhat larger than the value 0.99 Å reported in the literature as the covalent radius of Cl.[14] This fact may suggest some degree of ionicity of Cl. Alternatively, the increase agrees approximately with application of Pauling's rule[15] for the dependence of bond length on bond number. For fractional bond numbers this dependence is $-0.60\log n$, where n is the bond number, which gives an increase in bond length of the effective Cl radius of 0.36 Å for $n=\frac{1}{4}$. The electronegativity correction could then reduce this value by 0.1 Å, although the coefficient to be used is not fixed by Pauling's rules.[16]

TABLE I. Relation between the muffin-tin radius (MTR) used to calculate the Cl potential and the hard-sphere radius (HSR) found with such potential for the structure that produces best agreement with experiment.

MTR (Å)	d_z^S (Å)	HSR (Å)
0.93	1.57	1.13
1.23	1.72	1.23
1.325	1.78	1.26

*Sponsored in part by the NSF for the U. S.-Italy Cooperative Science Program and by the Consiglio Nazionale delle Ricerche.

†On leave of absence from the University of Florence, Florence, Italy.

[1]M. Lazzari, Electrochim. Metallorum 4, 453 (1967).
[2]R. Wilken and E. Menzel, Z. Naturforsch. A 28, 1914 (1973).
[3]R. G. Meisenheimer and J. N. Wilson, J. Catal. 1, 151 (1962).
[4]P. A. Kilty, N. C. Rol, and W. M. H. Sachter, in *Catalysis*, edited by J. W. Hightower (North-Holland, Amsterdam, 1973), p. 929.
[5]G. Rovida and F. Pratesi, Surf. Sci. 51, 270 (1975).
[6]G. Rovida and F. Pratesi (private communication).
[7]D. W. Jepsen and P. M. Marcus, in *Computational Methods in Band Theory*, edited by P. M. Marcus, J. F. Janak, and A. R. Williams (Plenum, New York, 1971), pp. 416–443.
[8]D. W. Jepsen, P. M. Marcus, and F. Jona, Phys. Rev. B 8, 5523 (1973).
[9]J. E. Demuth, D. W. Jepsen, and P. M. Marcus, J. Phys. C 8, L25 (1975).
[10]K. O. Legg, F. P. Jona, D. W. Jepsen, and P. M. Marcus, J. Phys. C 8, L492 (1975).
[11]M. A. Van Hove and S. Y. Tong, Surf. Sci. 52, 673 (1975).
[12]H. D. Shih, F. Jona, D. W. Jepsen, and P. M. Marcus (unpublished).
[13]The effects of different adsorbate potentials on LEED intensity calculations have been investigated by a few workers for a few systems [see Refs. 9 and 11, as well as J. E. Demuth, D. W. Jepsen, and P. M. Marcus, Solid State Commun. 13, 1311 (1973)] but not in terms of the dependence of structural parameters upon the muffin-tin radius of the adsorbate between the lower and upper limits as defined above.
[14]L. Pauling, *The Nature of the Chemical Bond* (Cornell University, Ithaca, New York, 1960), p. 224.
[15]Ref. 14, p. 255.
[16]Ref. 14, p. 229.

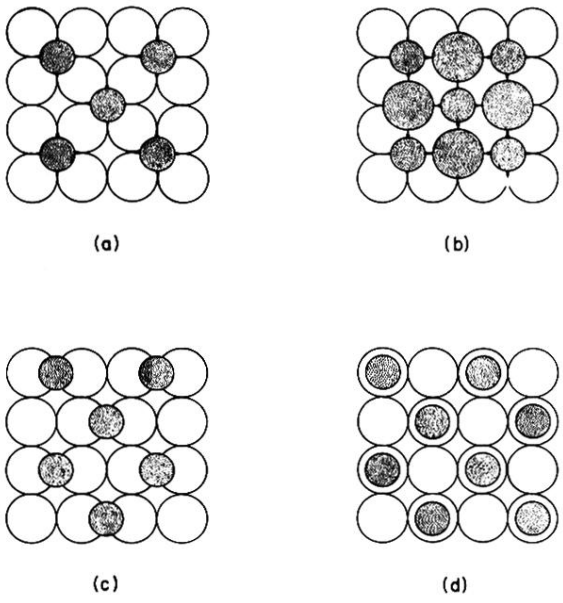

FIG. 1. Schematic models of the $c(2\times2)$ structures assumed for the calculations. (a) Overlayer with Cl in fourfold symmetrical sites; (b) Ag-Cl mixed layer; (c) Overlayer with Cl in bridge sites (one of two domains); (d) Overlayer with Cl in top sites. Shaded circles: overlayer or mixed-layer atoms. Open circles: Substrate Ag atoms.